Supporting Information

Bulkley et al. 10.1073/pnas.1008685107

SI Text

In addition to what was already mentioned in *Discussion* in the main article, a number of additional mutations in the 23S rRNA can alter the shape or interacting surface of the chloramphenicol binding site. For instance, an A2451U mutation effectively loosens the binding pocket of chloramphenicol by reducing the hydrophobic surface formed by the base of A2451 directly above the nitrobenzyl ring of chloramphenicol. Two other mutations, C2452A and U2504C, disrupt the U-C mismatch between A2452 and U2504, presumably altering the orientation of the base at position 2452 upon which the nitrobenzyl ring of chloramphenicol stacks (Fig. 1). Finally, the mutation A2503C has been shown to induce chloramphenicol resistance. The base at this position lies near the dichloro terminus of chloramphenicol and stacks with nearby bases of A2059 and G2061; when mutated from A to C, a majority of the hydrophobic contact with the base of G2061 will be lost, potentially leading to a local rearrangement of ribosomal RNA.

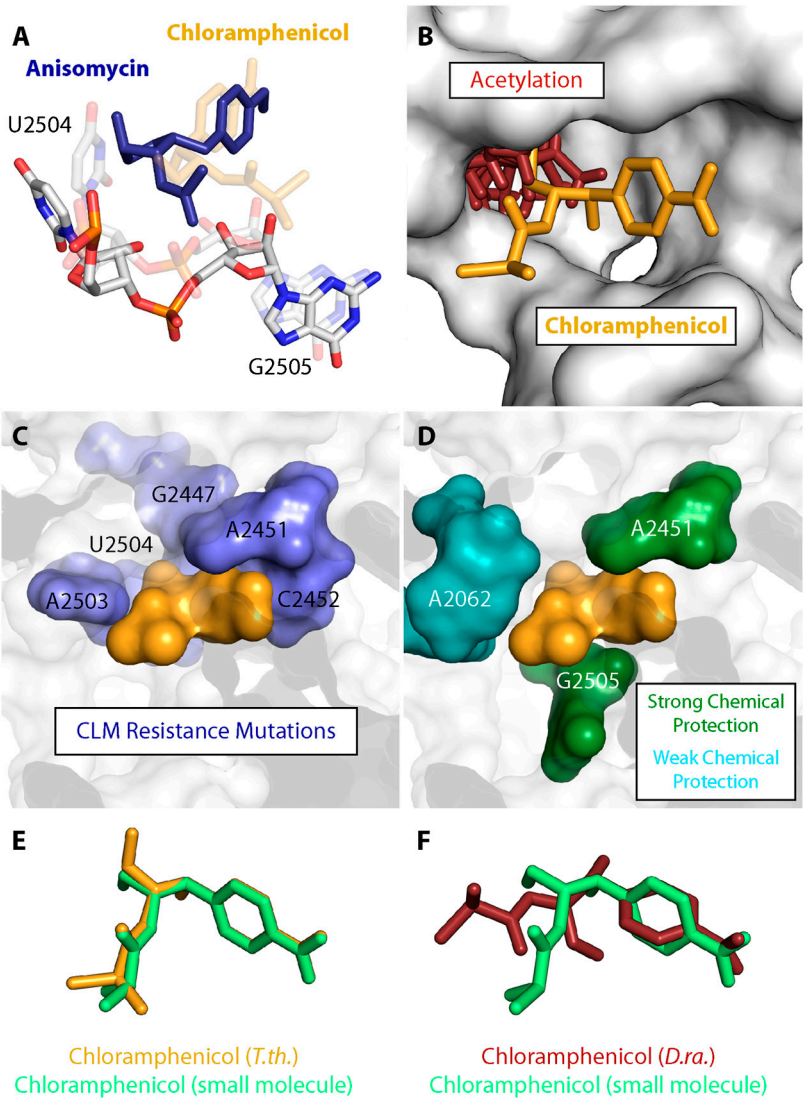

Fig. S1. Evaluation of chloramphenicol binding. (*A*) Comparison of the anisomycin and chloramphenicol binding pockets. Anisomycin (solid blue) bound to the *H.ma.* 50S (solid white) contrasts with chloramphenicol (transparent orange) bound to the *T.th.* 70S (transparent white). (*B*) Steric clashes created by acetylation of chloramphenicol at the methylene hydroxyl position. The unmodified drug (orange) and a range of possible orientations for the acetyl moiety (red) are shown. (*C*) Mutations leading to chloramphenicol resistance (1, 2). Chloramphenicol (orange surface) along with bases whose mutation have been linked to chloramphenicol resistance (purple surface) are shown. (*D*) Chemical protection by chloramphenicol (3, 4). Bases whose protection is strongly modified by chloramphenicol (green surface) along with bases whose protection is weakly modified by chloramphenicol(turquoise surface) are shown with chloramphenicol (orange surface). (*E*) Overlay of the chloramphenicol small molecule crystal structure (green) with the chloramphenicol model from the *T.th.* 70S complex (orange). (*F*) Overlay of the chloramphenicol small molecule crystal structure (green) with the chloramphenicol model from the *D.ra.* 50S complex (red).

1. Kearsey SE, Craig IW (1981) Altered ribosomal RNA genes in mitochondria from mammalian cells with chloramphenicol resistance. *Mol Cell* 290:607–608.
2. Blanc H, et al. (1981) Mitochondrial DNA of chloramphenicol-resistant mouse cells contains a single nucleotide change in the region encoding the 3′ end of the large ribosomal RNA. *Proc Natl Acad Sci USA* 78:3789–3793.
3. Moazed D, Noller HF (1987) Chloramphenicol, erythromycin, carbomycin and vernamycin B protect overlapping sites in the peptidyl transferase region of 23S ribosomal RNA. *Biochimie* 69:879–884.
4. Rodriguez-Fonseca C, et al. (1995) Fine structure of the peptidyl transferase centre on 23 S-like rRNAs deduced from chemical probing of antibiotic-ribosome complexes. *J Mol Biol* 247:224–235.

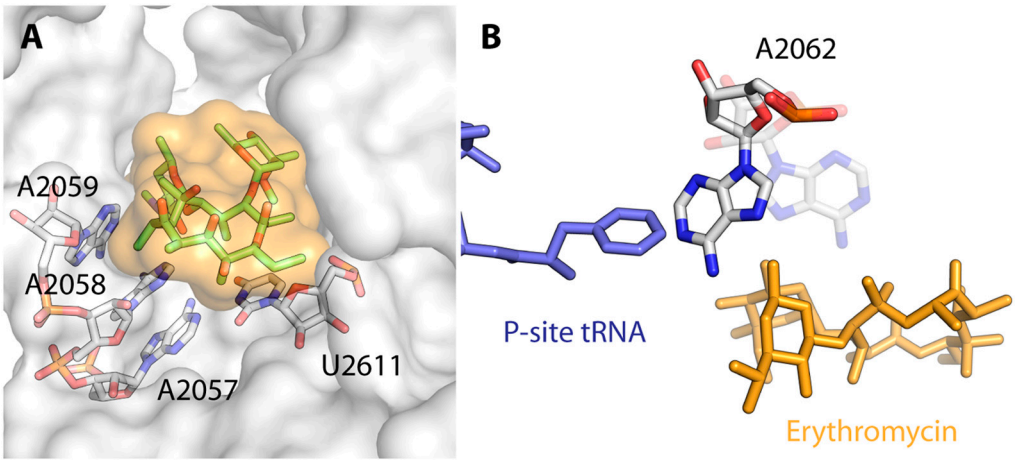

Fig. S2. Erythromycin interactions. (*A*) Erythromycin (green sticks, yellow surface) rests on a surface formed by bases of the exit tunnel (white sticks). (*B*) Movement of A2062 caused by erythromycin binding. Without erythromycin bound, A2062 (transparent white stick) points toward the terminus of the exit tunnel. When erythromycin binds, A2062 (solid white stick) moves toward the P site, coming within van der Waals contact of the P-site tRNA (1).

1. Voorhees RM, et al. (2009) Insights into substrate stabilization from snapshots of the peptidyl transferase center of the intact 70S ribosome. *Nat Struct Mol Biol* 16:528–533.

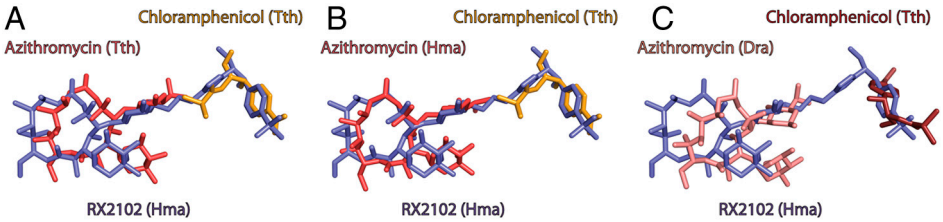

Fig. S3. Comparison among azithromycin, chloramphenicol, and RX2102 complexes with the ribosome. All structures were aligned on the basis of 23S ribosomal RNA. (*A*) Superposition of azithromycin and chloramphenicol complexed with the *T.th.* 70S ribosome (this work) and RX2102 complexed with the *H.ma.* 50S ribosome (PDB ID code 3OW2). (*B*) Superposition of azithromycin bound to the *H.ma.* 50S ribosome (1), chloramphenicol bound to the *T.th.* 70S ribosome and RX2102 bound to the *H.ma.* 50S. (*C*) Superposition of chloramphenicol and azithromycin bound to the *D.ra.* 50S (2, 3) and RX2102 bound to the *H.ma.* 50S.

1. Hansen JL, et al. (2002) The structures of four macrolide antibiotics bound to the large ribosomal subunit. *Mol Cell* 10:117–128.
2. Schlunzen F, et al. (2001) Structural basis for the interaction of antibiotics with the peptidyl transferase centre in eubacteria. *Nature* 413:814–821.
3. Schlunzen F, et al. (2003) Structural basis for the antibiotic activity of ketolides and azalides. *Structure* 11:329–338.

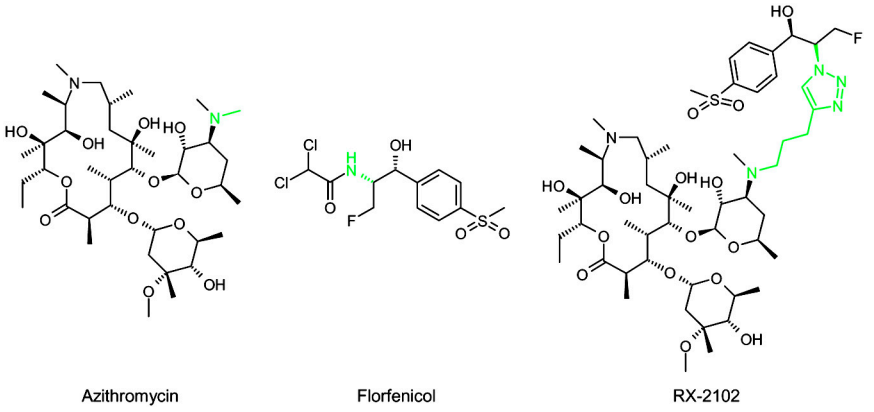

Fig. S4. Two-dimensional structures of parent antibiotics and RX2102 chimera.

Table S1. Data collection and refinement statistics

	Ery	Azi	Tel	Cam
Unit cell dimensions (*Space group*: $P2_12_12_1$)				
a	210 Å	210 Å	207 Å	210 Å
b	448 Å	450 Å	438 Å	448 Å
c	620 Å	625 Å	615 Å	621 Å
Data processing				
Resolution	40.0–3.1 (3.16–3.08)	40.0–3.2 (3.25–3.16)	40.0–3.2 (3.27–3.18)	40.0–3.2 (3.28–3.20)
R_{merge}	26.7 (122.8)	20.5 (92.2)	18.2 (89.1)	31.6 (141.8)
$\langle I/\sigma I \rangle$	8.08 (1.32)	7.46 (1.68)	8.16 (1.45)	7.73 (1.27)
Completeness	99.8 (99.9)	99.8 (99.7)	91.3 (86.3)	98.76 (99.2)
Redundancy	10.1 (10.1)	13.5 (3.8)	12.4 (7.0)	5.0 (5.3)
Refinement				
R_{work}	24.28	23.48	24.56	24.42
R_{free}	27.79	26.93	28.45	28.12
Bond dev.	0.01 Å	0.01 Å	0.01 Å	0.01 Å
Angle dev.	1.11°	1.12°	1.13°	1.13°

Table S2. Antibacterial activity (minimum inhibitory concentrations, in μg/mL) for parent antibiotics and chimera

S. pneumoniae strain	Resistance phenotype	Azithromycin	Florfenicol	RX-2102
ATCC49619 QC	Susceptible	≤0.25	2	≤0.25
96-018535	A2058G	≥128	2	0.5
02J1258	ErmB (2058 mono-methylation) + L4 (protein mutation)	≥128	2	1